EDDINGTON LIMIT AND RADIATIVE TRANSFER IN HIGHLY INHOMOGENEOUS ATMOSPHERES

Mateusz Ruszkowski and Mitchell C. Begelman[1]
JILA, Campus Box 440, University of Colorado, Boulder CO 80309-0440
mr@quixote.colorado.edu; mitch@jila.colorado.edu
Draft version February 1, 2008

ABSTRACT

Radiation dominated accretion disks are likely to be subject to the "photon bubble" instability, which may lead to strong density inhomogeneities on scales much shorter than the disk scale height. Such disks – and magnetized, radiation-dominated atmospheres in general – could radiate well above the Eddington limit without being disrupted. When density contrasts become large over distances of order the photon mean free path, radiative transfer cannot be described adequately using either the standard diffusion approximation or existing prescriptions for flux-limited diffusion. Using analytical and Monte Carlo techniques, we consider the effects of strong density gradients deep within radiation- and scattering-dominated atmospheres. We find that radiation viscosity – i.e., the off-diagonal elements of the radiation stress tensor – has an important effect on radiative transfer under such conditions. We compare analytical and numerical results in the specific case of a plane-parallel density wave structure and calculate Eddington enhancement factors due to the porosity of the atmosphere. Our results can be applied to the study of dynamical coupling between radiation forces and density inhomogeneities in radiation dominated accretion disks in two or three dimensions.

Subject headings: radiative transfer – accretion, accretion disks – stars: atmospheres – methods: analytical, numerical

1. INTRODUCTION

Radiation-dominated atmospheres of accretion disks and massive stars permeated by a moderately strong magnetic field are susceptible to the "photon bubble" instability (Arons 1992; Gammie 1998; Begelman 2001). In this process, high density regions tend to be pulled downward along the field lines and low density regions are pushed upward by radiation forces. The gas elements accelerated by radiation forces enter density maxima, where radiation forces decrease, and then progress downward again completing the cycle. Because subsequent acceleration episodes are increasingly large and magnetic tension prevents high density regions from spreading sideways, the density contrast increases. This leads to density inhomogeneities on scales shorter than the characteristic scale height of the accretion disk or stellar atmosphere. Under such conditions, radiation tends to bypass high density regions and travel more freely through tenuous ones. If the low- and high-density regions are dynamically coupled and most of the mass is in the high density phase, then the flux necessary to support the atmosphere against gravity can exceed Eddington limit. Photon bubble instability may be applicable to objects suspected of having super-Eddington luminosities, such as "ultraluminous X-ray sources" (Begelman 2002) and narrow-line Seyfert 1 galaxies (King and Puchnarewicz 2002). It has also been argued that the instability may occur in simple non-magnetized Thomson atmospheres as they approach the Eddington limit (Shaviv 2001b). The origin of this instability and the statistical properties of the inhomogeneities, such as their size relative to the size of the atmosphere, are different than that predicted by the magnetic photon bubble instability. This mechanism has been invoked to explain the discrepancy between relatively high outburst luminosities and relatively low outflow velocities in novae (Shaviv 1998, 2000, 2001a).

Radiative transfer in a medium where parts of the gas are optically thin, such as the upper regions of atmospheres in particular, cannot be treated using the standard diffusion approximation. The application of this approximation in the optically thin regime may lead to the radiation propagation rate exceeding the free-streaming rate $|\mathbf{F}| = cu$, where $\mathbf{F}$ and u are the radiation flux and energy density, respectively. Previous work on radiative transfer under such conditions focused on the development of flux-limited diffusion approximations (e.g., Levermore and Pomraning (1981); Melia and Zylstra (1991); Anile and Romano (1992)). A serious limitation of these methods is that they are applicable only in cases where the angular distribution of the specific intensity is a slowly varying function of space and time.

In this paper, we focus on radiative transfer deep within atmospheres (i.e., at high optical depth), where the effects of flux-limited diffusion are less important. But we consider the case where large density gradients – on scales of order the photon mean free path – lead to rapid fluctuations in the angular distribution function. It is easy to see why the standard diffusion approximations (with or without flux-limiting) fail under these circumstances. The standard diffusion approach predicts that the flux responds instantaneously to local changes in density. But in reality the flux can only respond to inhomogeneities provided that the density changes on scales much larger than the photon mean free path. When density inhomogeneities are optically thin, radiation does not "see" any

---

[1] Also at Department of Astrophysical and Planetary Sciences, University of Colorado

density contrasts. Using a simple ansatz, we have derived a modified diffusion equation and show that the effects of "photon viscosity" (i.e., off-diagonal elements of the radiation stress tensor) play an important role in radiative transfer in this case. Using analytical and Monte Carlo techniques we find that our analytical approach is much more accurate than standard diffusion or multi-stream approximations. Our results can be applied to the study of dynamical coupling between radiation forces and density inhomogeneities in radiation-dominated accretion disks.

The structure of this paper is as follows. In section 2 we discuss three-dimensional radiative transfer and show that the "photon viscosity" terms are important. In section 3 we constrain ourselves to the case of periodic, planar density waves embedded deep within an atmosphere and derive the corresponding Eddington enhancement factors under the assumption of global dynamical equilibrium. In section 4 we compare analytical formulas with Monte Carlo calculations and discuss our results. We propose that our method could be incorporated into existing radiation hydrodynamics codes such as the RHD module for ZEUS developed by Turner and Stone (2001).

2. RADIATIVE TRANSFER IN AN INHOMOGENEOUS ATMOSPHERE

We consider radiative transfer within infinite highly inhomogeneous atmospheres where the effects of flux-limited diffusion are very much reduced. Moreover, in a porous atmosphere, the radiation diffusion timescale is most likely much shorter than the characteristic gas dynamical timescale, i.e., radiation is probably not trapped by the motion of gaseous inhomogeneities (Begelman 2001). Therefore, for the purpose of calculating radiative transfer, we can neglect the time-dependence and motion of the gas distribution. We approximate the intensity distribution as

$$I(\mathbf{x}, \hat{\Omega}) = I_0(\mathbf{x}, \hat{\Omega}) + \frac{3}{4\pi}\hat{\Omega} \cdot \mathbf{F}(\mathbf{x}), \qquad (1)$$

where $\mathbf{F}$ is the local flux vector, $\hat{\Omega}$ is the directional unit vector, and $\mathbf{x}$ is the position vector. This approximation means that the first nontrivial correction to intensity $I_0(\mathbf{x}, \hat{\Omega})$ is symmetric with respect to the direction defined by the *local* flux. This has to be contrasted with a familiar case of a plane-parallel atmosphere. In such a case, it is customary to assume that the directional distribution of intensity $I(\mathbf{x}, \hat{\Omega})$ is symmetric relative to the vertical direction which coincides with the direction of the flux vector. However, in the case of highly inhomogeneous atmosphere, radiation bypasses denser regions and the flux vector can rapidly change its orientation and only the volume-averaged flux is vertical. Thus, in our approach, the local "symmetry axis" is changing direction throughout the atmosphere and no global symmetry is required. We also assume that all the odd moments of I_0 vanish, i.e., $\int \hat{\Omega}_i I_0 d\Omega = \int \hat{\Omega}_i \hat{\Omega}_j \hat{\Omega}_k I_0 d\Omega = 0$, but otherwise make no assumptions about the directional dependence of I_0. The equation of radiative transfer for a 3D scattering atmosphere reads

$$\frac{1}{\sigma}\hat{\Omega} \cdot \nabla I = -I + \frac{1}{4\pi}\int I d\Omega, \qquad (2)$$

where $\sigma = \rho\kappa$ is the scattering coefficient. Taking zeroth and first moments of eq. (2) we obtain

$$\nabla \cdot \mathbf{F} = 0 \qquad (3)$$

and

$$\mathbf{F} = -\frac{c}{\sigma}\nabla \cdot \mathbf{T}, \qquad (4)$$

where $\mathbf{T}$ is the radiation stress tensor, the components of which are

$$T_{ij} = \frac{1}{c}\int \hat{\Omega}_i \hat{\Omega}_j I_0 d\Omega. \qquad (5)$$

The closure relation for T_{ij} in terms of F_i and $J \equiv \frac{1}{4\pi}\int I d\Omega$ can be obtained by calculating the second moment of eq. (2), assuming the form of the intensity given by eq. (1). This leads to the equation for the radiation stress tensor:

$$T_{ij} = \begin{cases} \frac{u}{3} - \frac{1}{5\sigma c}\left(\frac{\partial F_i}{\partial x^j} + \frac{\partial F_j}{\partial x^i}\right) & \text{for } i = j \\ -\frac{1}{10\sigma c}\left(\frac{\partial F_i}{\partial x^j} + \frac{\partial F_j}{\partial x^i}\right) & \text{for } i \neq j \end{cases} \qquad (6)$$

where $u = 4\pi J/c$ is the energy density and J is the mean intensity. Note that (i) the diagonal terms T_{ii} may be different from one another, and (ii) the off-diagonal elements of the radiation stress tensor do not vanish. The first point implies that this approach incorporates variable Eddington factors. The off-diagonal elements are responsible for "photon viscosity" and are non-zero even though bulk gas motions in the atmosphere were assumed to be negligible. This is because the "photon fluid" is moving through the gas, and may exert shear stresses. Substituting eq. (6) into eq. (4) and using eq. (3), we obtain:

$$F_i = -\frac{c}{3\sigma}\frac{\partial u}{\partial x^i} + \frac{1}{10\sigma^2}\left[\frac{\partial^2 F_i}{\partial x_j x^j} + 2\frac{\partial^2 F_i}{\partial x_i^2} - \frac{1}{\sigma}\frac{\partial \sigma}{\partial x_j}\left(\frac{\partial F_i}{\partial x^j} + \frac{\partial F_j}{\partial x^i}\right) - \frac{2}{\sigma}\frac{\partial \sigma}{\partial x^i}\frac{\partial F_i}{\partial x_i}\right]. \qquad (7)$$

In the above equation, summation is imposed *only* over repeated j indices. Equation (7) and equation (3) are the governing equations of radiative transfer in our approximation.

3. 2D DENSITY INHOMOGENEITIES

In order to illustrate our method, we now consider the simplified case of a plane-parallel wave density pattern (see Fig. 1). The scattering coefficient is assumed to be only a function of the distance ξ perpendicular to the slabs, i.e., $\sigma = \rho\kappa = \sigma(\xi)$ with $\xi = \mu x + (1-\mu^2)^{1/2}z$, where $\mu = \cos\psi$. We also assume that $\partial/\partial y = 0$ and that the components of flux depend only on ξ. We consider an atmosphere which is in *global* (i.e., volume-averaged) hydrostatic equilibrium, where radiation pressure balances gravity $-g\hat{z}$. This implies that the gradient of energy density must be of the form

$$\nabla u = u'(\xi)\nabla\xi - \frac{3\langle\sigma\rangle}{c}F_{\text{Edd}}\hat{z}, \qquad (8)$$

where a prime denotes differentiation with respect to ξ, $\langle\sigma\rangle$ is the volume average of the scattering coefficient, and $F_{\text{Edd}} = gc/\kappa$ is the Eddington flux. From equation (7) and equation (3) we obtain:

$$\mu F_z - (1-\mu^2)^{1/2} F_x = \mu \frac{\langle\sigma\rangle}{\sigma} F_{\text{Edd}} + \frac{1}{\alpha^2 \sigma \mu} \left(\frac{F_z'}{\sigma}\right)', \quad (9)$$

where $\alpha^2(\mu) = 10/(1 + 4\mu^2 - 4\mu^4)$. Integrating eq. (3) over ξ we obtain

$$\mu F_x + (1-\mu^2)^{1/2} F_z = const \equiv (1-\mu^2)^{1/2} F_0, \quad (10)$$

where F_0 is the integration constant. Using eq. (10) to eliminate F_x from eq. (9) we get

$$F_z = (1-\mu^2) F_0 + \mu^2 \frac{\langle\sigma\rangle}{\sigma} F_{\text{Edd}} + \frac{1}{\alpha^2 \sigma} \left(\frac{F_z'}{\sigma}\right)'. \quad (11)$$

Multiplying equation (11) by σ and then volume-averaging it and demanding that the solution be bounded, we have

$$\langle\sigma\rangle F_{\text{Edd}} = \langle\sigma F_z\rangle = (1-\mu^2)\langle\sigma\rangle F_0 + \mu^2\langle\sigma\rangle F_{\text{Edd}}, \quad (12)$$

where the first equality in equation (12) comes from the requirement that the atmosphere be in global hydrostatic equilibrium. Therefore, $F_0 = F_{\text{Edd}}$ and the final equation for the vertical flux is

$$F_z = \left(1 - \mu^2 + \mu^2 \frac{\langle\sigma\rangle}{\sigma}\right) F_{\text{Edd}} + \frac{1}{\alpha^2 \sigma} \left(\frac{F_z'}{\sigma}\right)'. \quad (13)$$

3.1. Eddington enhancement factor

Using equation (13) we can now calculate the Eddington enhancement factor $l \equiv \langle F_z/F_{\text{Edd}}\rangle$. We can simplify and non-dimensionalize equation (13) by defining

$$f \equiv \frac{F_z}{F_{\text{Edd}}} - (1-\mu^2). \quad (14)$$

Thus, the Eddington factor is

$$l \equiv (1-\mu^2) + \langle f\rangle, \quad (15)$$

where $\langle f\rangle$ is the volume average of f. Defining optical depth $d\tau = \sigma d\xi$, letting the prime now denote differentiation with respect to τ, and normalizing the scattering coefficient to its mean value (i.e. $\sigma \rightarrow \sigma/\langle\sigma\rangle$), we obtain a simplified form of equation (13)

$$f'' - \alpha^2 f = -\frac{\alpha^2 \mu^2}{\sigma}. \quad (16)$$

We now consider a periodic slab model in which the scattering coefficient is given by:

$$\sigma = \begin{cases} \sigma_1 & \text{if } -\tau_1 < \tau < 0, \text{ region 1} \\ \sigma_2 & \text{if } \quad 0 < \tau < \tau_2, \text{ region 2} . \end{cases} \quad (17)$$

The solutions to equation (16) in regions 1 and 2 are

$$f_{1,2}(\tau) = a_{1,2} \sinh(\alpha\tau) + b_{1,2} \cosh(\alpha\tau) + \frac{\mu^2}{\sigma_{1,2}}, \quad (18)$$

where $a_{1,2}$ and $b_{1,2}$ are the integration constants. Functions f and f' have to be continuous across each slab boundary. Therefore the matching conditions are:

$$f_1(0) = f_2(0), \quad f_1'(0) = f_2'(0) \quad (19)$$
$$f_1(-\tau_1) = f_2(\tau_2), f_1'(-\tau_1) = f_2'(\tau_2). \quad (20)$$

Using the above matching conditions to derive the integration constants $a_{1,2}$ and $b_{1,2}$ and then volume averaging the solution for f, we obtain the expression for $\langle f\rangle$

$$\langle f\rangle = \frac{\mu^2\langle\sigma\rangle}{\xi_1 + \xi_2} \left[\frac{\xi_1}{\sigma_1} + \frac{\xi_2}{\sigma_2} - \frac{2}{\alpha} \frac{(\Delta\sigma)^2}{\sigma_1^2 \sigma_2^2} \frac{\sinh x \sinh y}{\sinh(x+y)}\right], \quad (21)$$

where $x = \alpha\tau_1/2$, $y = \alpha\tau_2/2$, $\Delta\sigma = \sigma_2 - \sigma_1$, and $\xi_{1,2} = \tau_{1,2}/\sigma_{1,2}$. The Eddington enhancement factor l follows directly from equations (21) and (15).

4. COMPARISON WITH MONTE CARLO SIMULATIONS

We now compare our analytical results with Monte Carlo simulations. The setup of the numerical experiment was as follows. We instantaneously injected a large number of photons in the equatorial plane (i.e., $z = 0$) of a very flat, three-dimensional box (i.e., $z \in [-z_o, z_o]$; $x, y \in [-w_o, w_o]$, where $z_o \ll w_o$). Densities and height of the computational box were chosen in such a way as to assure that the optical thickness in the vertical direction would always be large throughout the box. The initial photon angular distribution was uniform. Although we included the anisotropy due to the Thomson scattering cross section, we found this effect to have no influence on our final results. We followed the trajectories of all photons and calculated photon travel times between scatterings. Momentum transfer for every scattering was calculated using the method of weights (Pozdnyakov at al. 1983). We then computed the force exerted on the atmosphere as a function of the time delay following the instantaneous photon injection. Of course, as photons diffuse out of the atmosphere, the force exerted on the gas gradually declines. Therefore, the total force, corresponding to a continuous photon flux, was calculated by superposing many such time-dependent force distributions due to groups of photons injected (instantaneously) at uniform time intervals. The total force exerted on the atmosphere was characterized by a gradual increase with time followed by a flat maximum. The Eddington enhancement factor is then given by the ratio of the "saturated" total force (i.e., total, constant force at late times) exerted on a homogeneous atmosphere, to the total force acting on an inhomogeneous atmosphere characterized by the same mean density. Note that the Eddington enhancement factor, defined in this way, can also be interpreted as *the ratio of fluxes necessary to exert the same amount of force on an inhomogeneous atmosphere as on the corresponding homogeneous atmosphere.* This ratio is the same even if the homogeneous atmosphere is sub-Eddington, i.e., is only partially supported against gravity by radiation.

Figure 2 shows the Eddington enhancement factor for variable inclination of slabs (upper panels) and for changing density contrast of vertical slabs (lower panels). In all cases, the Thomson depth of the high density slabs τ_h is constant but the optical depth across low density regions increases from values $\tau_l < 1$ to $\tau_l > 1$ from left to right (see caption of Fig. 2 for more details). As expected, the Eddington factor increases as the slabs rotate toward the vertical direction because the atmosphere effectively becomes more porous (see upper panels). When the slabs are vertical, the flux enhancement factor increases as the

density contrast σ_h/σ_l becomes larger for constant mean density. This is due to the fact that the volume filling factor of the high-density gas decreases while that of the low-density gas increases, but the respective masses of the two density phases remain the same. Therefore, the mean, volume-weighted, flux is

$$\langle F \rangle = (1 - f_v)F_l + f_v F_h \approx F_l, \qquad (22)$$

where f_v is the volume filling factor of the dense gas and F_l and F_h are the fluxes propagating through tenuous and dense regions, respectively. As the density contrast increases and f_v decreases, radiation tends to "flow" primarily through the low density channels and, therefore, more flux is necessary to exert the same total force as in the homogeneous case because radiation interacts less efficiently with tenuous gas. Quantitatively, in the diffusion limit, we have (Shaviv 1998)

$$l = \langle \rho \rangle \left\langle \frac{1}{\rho} \right\rangle = \left(\frac{\xi_l}{\sigma_l} + \frac{\xi_h}{\sigma_h} \right) \frac{\langle \sigma \rangle}{\xi_l + \xi_h}. \qquad (23)$$

When most volume is in the low-density phase but most mass is in the high-density phase (i.e., $f_v \to 0$ or $\xi_h/\xi_l \to 0$), then $l \approx f_v \rho_h/\rho_l$ if $f_v \gg \rho_l/\rho_h$. This qualitatively explains why l decreases with $\tau_l \geq 1$ at constant density contrast σ_h/σ_l (cf. third and fourth columns on Fig. 2). At small optical depth τ_l, equation (23) would lead to very inaccurate answers. For example, equation (23) predicts $l \sim 23$ for vertical slabs with $\tau_l = 0.1$ and $\sigma_h/\sigma_l = 100$, compared to the actual value $l \sim 5$ and our analytic result ~ 4 from eq. (21) (cf. lower left panel). This discrepancy is due largely to neglect of the anisotropy of the radiation field, whereas our approach gives much more accurate results even in such an extreme case. Moreover, note that the "anisotropy term" in our expression for the flux enhancement factor, which is proportional to $(\Delta\sigma)^2 = (\sigma_h - \sigma_l)^2$, vanishes for large Thomson depths and thus equations (21) and (15) reduce to equation (23) in the diffusion limit. We also considered "multi-stream" approximation schemes in order to account for the radiation anisotropy, but found the "intensity moment" approach developed here to be in significantly better agreement with Monte Carlo simulations.

5. SUMMARY

We have considered radiative transfer deep within extremely inhomogeneous atmospheres, and have demonstrated that, under such conditions, radiation viscosity – i.e., the off-diagonal elements of the radiation stress tensor – plays an important role. Our approach is significantly more accurate than approaches based on the diffusion equation and multi-stream approximation. The technique developed here can be applied to the nonlinear evolution of radiation-driven instabilities in accretion disks. In particular, it can be used to study the dynamical coupling of matter and radiation in order to determine the characteristic length scales and density contrasts arising from "photon bubble" instability. This, in turn, will permit a self-consistent determination of the magnitude of the Eddington enhancement factor in radiation-dominated accretion disks. We also suggest that our method could be incorporated into radiation hydrodynamics codes such as the RHD module for ZEUS (Turner and Stone 2001).

REFERENCES

Arons, J. 1992, ApJ, 388, 561
Anile, A.M. and Romano, V. 1992, ApJ, 386, 325
Begelman, M.C. 2001, ApJ, 551, 897
Begelman, M.C. 2002, ApJ, 568, L97
Gammie, C.F. 1998, ApJ, 297, 929
Levermore, C.D. and Pomraning, G.C. 1981, ApJ, 248, 321 (LP)
Melia, F. and Zylstra G.J. 1991, ApJ, 374, 732

Pozdnyakov, L.A., Sobol, I.M. and Sunyaev, R.A. 1983, ASPRv, v.2, 189
King A.R. and Puchnarewicz, E.M. 2002, preprint
Shaviv, N. 1998, ApJ, 494, L193
Shaviv, N. 2000, ApJ, 532, L137
Shaviv, N. 2001a, MNRAS, 326, 126
Shaviv, N. 2001b, ApJ, 549, 1093
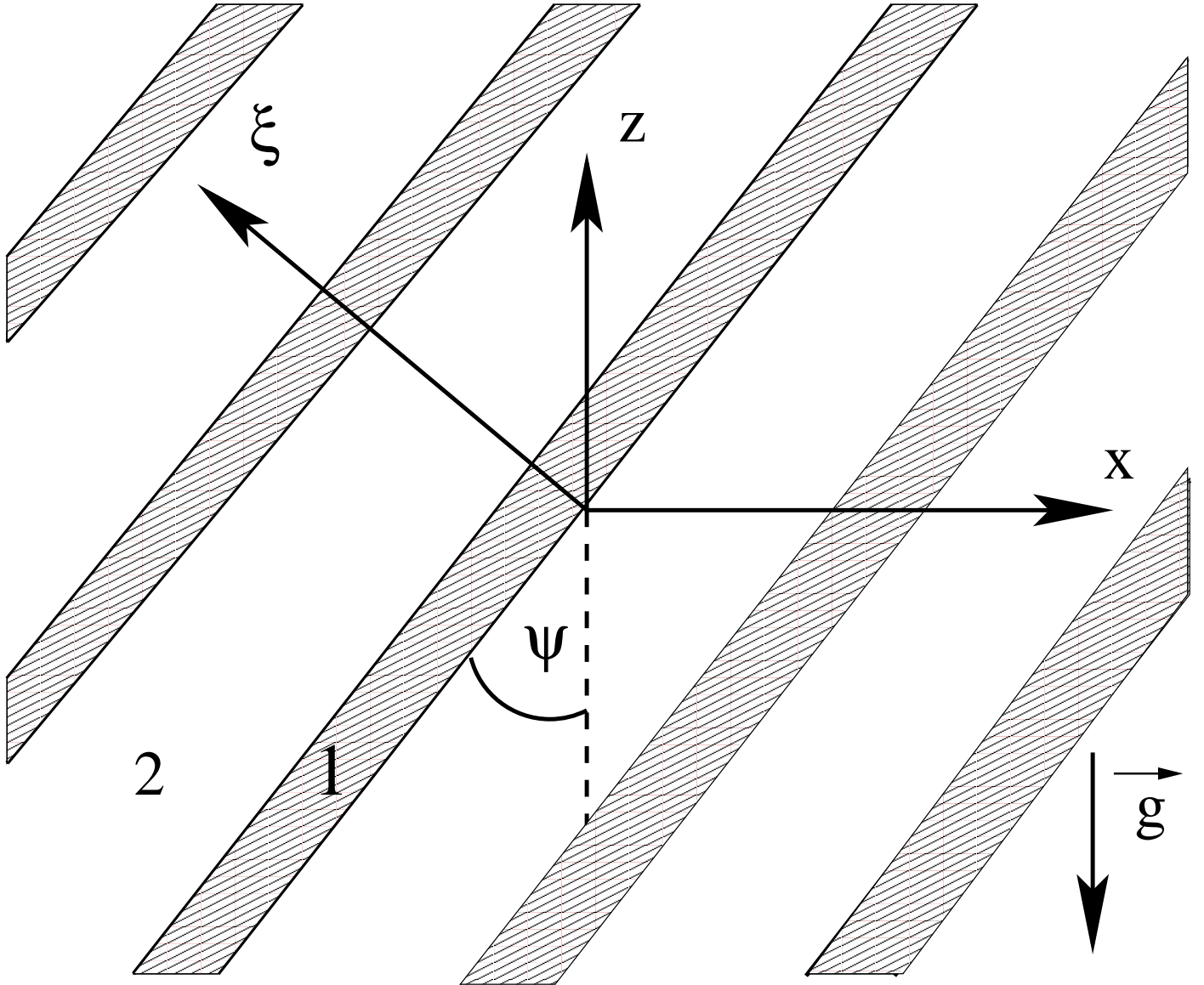Turner N.J., and Stone J.M. 2001, ApJS, 135, 95

Fig. 1.— Density structure of an inhomogeneous atmosphere. Shaded and unshaded zones denote higher and lower density regions, respectively. The region shown is much smaller than the overall radiation pressure scale height $\left|\frac{u}{\nabla u}\right|$.
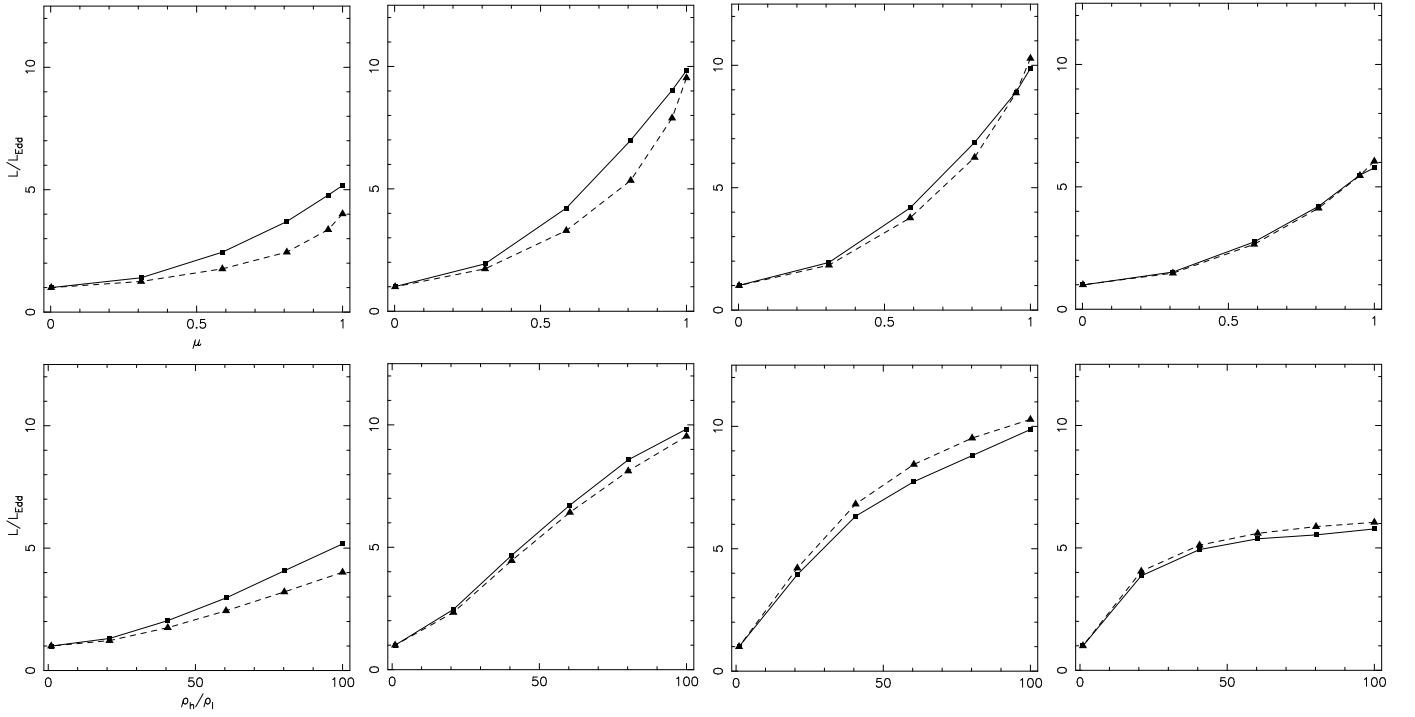
FIG. 2.— Eddington enhancement factors $L/L_{\rm Edd}$ for $\tau_h = 20$ and $\tau_l = 0.10$, 0.33, 1.00, 3.00 (from left to right column, respectively). Upper panels show $L/L_{\rm Edd}$ as a function of $\mu = \cos\psi$ for scattering coefficients of low and high density regions equal to $\sigma_l = 10$ and $\sigma_h = 1000$, respectively. Lower panels show $L/L_{\rm Edd}$ as a function of σ_h/σ_l for vertical slabs. Dashed lines show analytical predictions from equations (15) and (21), while solid lines show results from Monte Carlo simulations.